iScience

CellPress

Article

Sequential Solution Polymerization of Poly(3,4-ethylenedioxythiophene) Using V_2O_5 as Oxidant for Flexible Touch Sensors

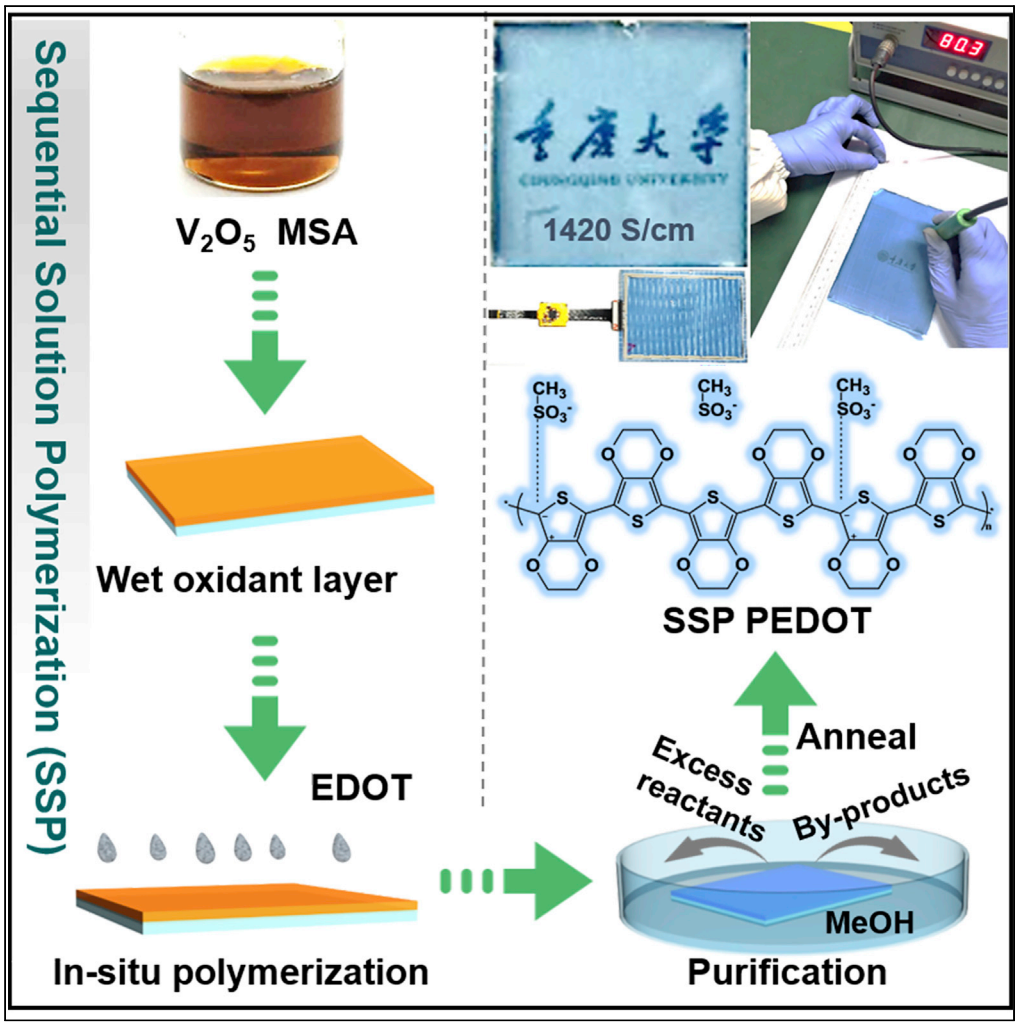

Rui Chen, Kuan Sun, Qi Zhang, ..., Chi Ma, Yiyang Zhang, Jianyong Ouyang

kuan.sun@cqu.edu.cn (K.S.)
mseoj@nus.edu.sg (J.O.)

HIGHLIGHTS

Sequential solution polymerization (SSP) of PEDOT film delivers high conductivity

The SSP method is compatible with large-scale printing technologies

Touch sensor made with SSP PEDOT exhibits superior flexibility and sensitivity

Chen et al., iScience 12, 66–75
February 22, 2019
https://doi.org/10.1016/j.isci.2019.01.003

iScience

CellPress

Article

Sequential Solution Polymerization of Poly(3,4-ethylenedioxythiophene) Using V_2O_5 as Oxidant for Flexible Touch Sensors

Rui Chen,[1] Kuan Sun,[1,6,*] Qi Zhang,[1] Yongli Zhou,[1] Meng Li,[1] Yuyang Sun,[2] Zhou Wu,[2] Yuyang Wu,[3] Xinlu Li,[3] Jialei Xi,[4] Chi Ma,[4] Yiyang Zhang,[4] and Jianyong Ouyang[5,*]

SUMMARY

Various *in situ* synthesis methods have been developed for the polymerization of 3,4-ethylenedioxythiophene monomers, such as electropolymerization, oxidative chemical vapor deposition, and vapor phase polymerization. Meeting industrial requirements through these techniques has, however, proven challenging. Here, we introduce an alternative method to fabricate highly conductive poly(3,4-ethylenedioxythiophene) (PEDOT) films *in situ* by solution means. The process involves sequential deposition of oxidants (V_2O_5 in this case) and monomers. Excess reactants and by-products can be completely removed from the PEDOT film by MeOH rinsing. The obtained PEDOT films possess good crystallinity and high doping level, with carrier concentration three orders of magnitude higher than that of the commercial product (PH1000, Heraeus GmbH). The electrical conductivity of the as-cast PEDOT film reaches up to 1,420 S/cm. In addition, this method is fully compatible with large-scale printing techniques. These PEDOT conducting films enable the realization of flexible touch sensors, which demonstrate superior flexibility and sensitivity.

INTRODUCTION

Poly(3,4-ethylenedioxythiophene) (PEDOT) is a conjugated polymer with many attractive properties, such as good conductivity, high optical transparency in visible range, excellent flexibility, and good chemical stability. These properties render it a key component for transparent electrodes, electrochromic devices, electromagnetic shielding, etc.(Sun et al., 2015a, 2015c; Zhou et al., 2010; Dong et al., 2010; Xia et al., 2017) *In situ* polymerization of 3,4-ethylenedioxythiophene (EDOT) monomers is an approach to obtain PEDOT films. There are generally three methods, namely, electropolymerization (EP) (Syed ZainolAbidin et al., 2018), oxidative chemical vapor deposition (OCVD), and vapor phase polymerization (VPP) (Alf et al., 2010; Fabretto et al., 2009). In the EP process, the EDOT monomer is dissolved in electrolyte and then polymerized on an electrode under electrical bias (Schoetz et al., 2018; Syed ZainolAbidin et al., 2018). A conductive substrate is required in such a process, thus limiting the application of this method. In the OCVD process, the monomer and oxidant are delivered in vapor phase at the same time, making it possible to synthesize, deposit, and dope the conjugated polymer in a single step (Lee and Gleason, 2015; Alf et al., 2010). In contrast, VPP needs two steps: (1) forming an oxidant layer on the substrate by solution means, e.g., spin coating, dip coating, blade coating, etc. and (2) exposing the oxidant-covered substrate to monomer vapor (Bhattacharyya et al., 2012). In recent years, the VPP method has gained popularity in EDOT polymerization. Kim et al. first polymerized PEDOT film via VPP; they used $FeCl_3 \cdot 6H_2O$ as oxidant and the obtained PEDOT film exhibited a low conductivity of 1 S/cm at thickness ranging from 20 to 100 nm (Kim et al., 2003). Then Winther-Jensen et al. changed the oxidant to iron (III) *p*-toluenesulfonate, and the conductivity exceeded 1,000 S/cm with the addition of pyridine (Winther-Jensen and West, 2004). After that, different weak bases such as pyridine, imidazole, and glycol-based block copolymers such as poly(ethylene glycol)-block-poly(propylene glycol)-block-poly(ethylene glycol) (PEG-PPG-PEG) and poly(ethylene glycol)-*ran*-poly(propylene glycol) (PEG-ran-PPG) were added to the oxidant solution to adjust the polymerization rate and to inhibit side reactions, leading to highly conductive PEDOT films (Metsik et al., 2014; Huang and Chu, 2011; Zuber et al., 2008; Fabretto et al., 2009, 2012; Ouyang et al., 2018). Notably, Sung et al. obtained single crystalline PEDOT nanowires in nanoscale channels of a mold covered with $FeCl_3$, the average conductivity reached 7,629 S/cm, and the highest value was up to 8,797 S/cm (Cho et al., 2014). Although extremely high conductivity of PEDOT is demonstrated, the deposition rate and film homogeneity still cannot meet the industrial requirement. Therefore a faster and more controllable polymerization technique is highly desirable.

[1]MOE Key Laboratory of Low-grade Energy Utilization Technologies and Systems, School of Energy & Power Engineering, Chongqing University, Chongqing 400044, China

[2]MOE Key Laboratory of Dependable Service Computing in Cyber Physical Society, School of Automation, Chongqing University, Chongqing 400044, China

[3]School of Materials Science and Engineering, Chongqing University, Chongqing 400044, China

[4]Chengdu Mobius Technology, Sichuan 610015, China

[5]Department of Materials Science and Engineering, National University of Singapore, Singapore 117574, Singapore

[6]Lead Contact

*Correspondence: kuan.sun@cqu.edu.cn (K.S.), mseoj@nus.edu.sg (J.O.)

https://doi.org/10.1016/j.isci.2019.01.003

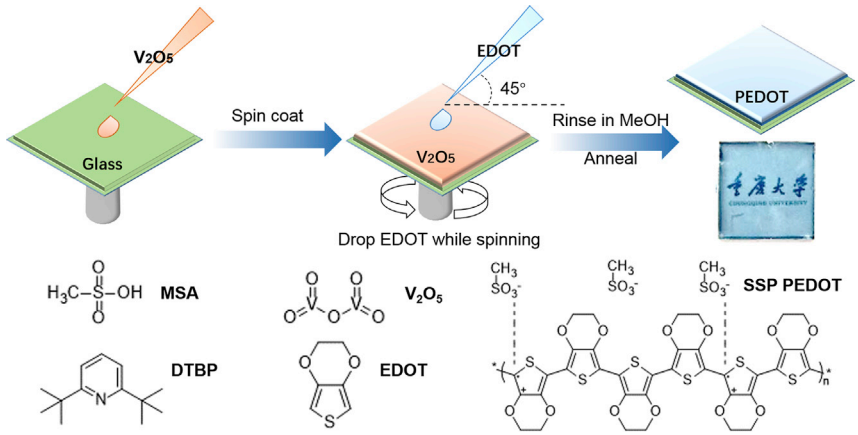

Scheme 1. Synthesis of PEDOT Film via Sequential Solution Polymerization (SSP)

Schematic diagram of the synthesis procedure of PEDOT film and chemical structure of methanesulfonic acid (MSA), vanadium pentoxide (V_2O_5), 2,6-di-tert-butylpyridine (DTBP), 3,4-ethylenedioxythiophene (EDOT), and its polymer PEDOT.

In most of the redox reactions of EDOT polymerization, Fe^{3+} acts as the electron acceptor. However, common oxidants like $FeCl_3$ and Fe(III) tosylate can crystallize easily, resulting in structural defects in the polymerized film (Fabretto et al., 2009; Shi et al., 2017). Vanadium pentoxide (V_2O_5) is known for its strong oxidizing property and high activity toward EDOT monomer (Murugan et al., 2001; Guo et al., 2015b). Zhang et al. synthesized PEDOT nanofibers using V_2O_5 as the oxidant at room temperature in a single step, and the conductivity was 15 S/cm, higher than that of pristine poly(3,4-ethylenedioxythiophene): poly(styrenesulfonate) (PEDOT:PSS) film (Zhang et al., 2005). V_2O_5 could change the morphology of PEDOT chains from granular to nanofibrillar for better electrical connectivity. Guo et al. synthesized layered V_2O_5/PEDOT nanowires in large scale by stirring the aqueous mixture of V_2O_5 powder and EDOT at room temperature (Guo et al., 2015a). V_2O_5 acted as both an oxidant and a template for EDOT polymerization. Therefore, V_2O_5 could be a good candidate for the polymerization of EDOT owing to its dual function of oxidizing and seeding template.

In this work, a novel and facile method, sequential solution polymerization (SSP), is introduced to fabricate highly conductive PEDOT films *in situ* by solution means in high throughput. As shown in Scheme 1, the process involves sequential deposition of a methanesulfonic acid (MSA) solution of V_2O_5 and 2,6-di-tert-butylpyridine (DTBP) as well as an acetonitrile (MeCN) solution of EDOT monomers (Benoit et al., 1988; Bashir et al., 2013). The whole process can be completed within a minute. The electrical conductivity of the PEDOT film can reach 1,420 S/cm, with an average value around 1,333 S/cm. Compared with the widely used commercial PEDOT:PSS (PH1000, Heraeus GmbH), the SSP PEDOT film has better crystallinity and higher doping level. Characterizations suggest that the SSP PEDOT films have comparable charge carrier mobility as PH1000, but three orders of magnitude higher carrier concentrations than PH1000. In addition, this process is compatible with large-scale printing techniques. A large-area (15 × 12 cm) PEDOT film is deposited successfully on polyethylene terephthalate (PET) film, and a low sheet resistance of 81 Ω/sq was obtained. The flexible SSP PEDOT film was applied to capacitive touch sensor, which showed favorable touch function and still worked well after folding it with a bending radius less than 1 mm. This new polymerization route paves the way to scalable deposition of conductive and homogeneous PEDOT films on flexible substrate.

RESULTS AND DISCUSSION

Polymerization of PEDOT Film via Sequential Solution Deposition

Scheme 1 shows the SSP process to deposit the PEDOT film. First, an MSA solution of V_2O_5 and DTBP is spin coated on glass substrate. Then an MeCN solution of EDOT is dropped onto the spinning oxidant-covered substrate. The whole process can be completed within a minute. Finally, the film is rinsed in MeOH to remove residuals and dried to form a solid film. The first precursor solution contains V_2O_5, MSA, and DTBP. Among them, V_2O_5 acts as the oxidant and seeding template for EDOT. MSA is employed to dissolve V_2O_5 and to drive the polymerization of EDOT (Winther-Jensen and West, 2004). To avoid

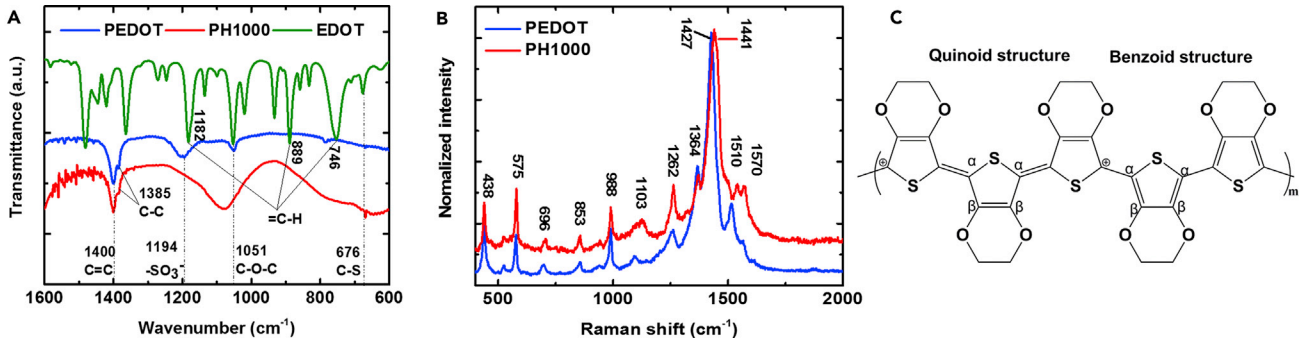

Figure 1. Identification of SSP PEDOT

(A) FTIR spectra of EDOT, PH1000, and SSP PEDOT.

(B) Raman spectra of PH1000 and SSP PEDOT.

(C) Benzoid or quinoid structure in a PEDOT chain.

uncontrollable polymerization and side reactions (Li and Ma, 2016; Winther-Jensen and West, 2004), a weak base (DTBP) is added to serve as a proton scavenger; meanwhile, it can also increase the viscosity of the precursor solution. Thus DTBP is able to adjust the polymerization rate and improve the film quality. The monomer solution consists of EDOT and MeCN solvent. EDOT is water insoluble; the type of solvent has a significant impact on the reaction rate and ultimate properties of the polymerized films. A polar organic solvent, MeCN, is chosen to improve the reaction activity of EDOT owing to its high polarity and low donor number (Bashir et al., 2013). The yellowish oxidant-covered substrate turns into light blue, which is the color of PEDOT, immediately when the monomer solution is dropped onto the surface, signifying the successful polymerization of EDOT.

To confirm that the EDOT monomers are polymerized into PEDOT, Fourier transform infrared spectroscopy (FTIR) is employed to compare the functional groups of SSP PEDOT, EDOT monomers, and PH1000. As shown in Figure 1A, the absorption bands around 1,364 cm^{-1} and 1,481 cm^{-1} in EDOT spectrum can be assigned to C-C and C=C bonds (Bahry et al., 2018; Loganathan and Pickup, 2005; Vaillant et al., 2006). They are shifted to 1,385 cm^{-1} and 1,400 cm^{-1} in SSP PEDOT and PH1000, implying that the conjugated structure is altered. In addition, the absorption band around 746 cm^{-1}, 889 cm^{-1}, and 1,182 cm^{-1} for =C-H in-plane and out-of-plane vibrations are found in the EDOT spectrum. However, they are absent in SSP PEDOT and PH1000, suggesting the successful polymerization due to the formation of α-α coupling (Coletta et al., 2016; Bahry et al., 2018; Ghosh et al., 2014). Furthermore, a characteristic peak for $–SO_3^-$ group is observed in SSP PEDOT, implying that MSA might exist in PEDOT film to act as counterions, similar to the role of PSS in PEDOT:PSS. Besides all these changes, a few peaks related to the monomer structure can also be found in SSP PEDOT. For example, the absorption bands for C-O-C stretching in ethylenedioxy group appeared on the spectra at 1,051 cm^{-1}(Bahry et al., 2018). The vibration modes of C-S bond in the thiophene ring can be observed at 676 cm^{-1}(Vaillant et al., 2006). These matched peaks indicate that the monomer unit of SSP PEDOT is still EDOT.

Figure 1B presents the Raman spectra of SSP PEDOT and PH1000 in a wave number range of 400–2,000 cm^{-1}. The spectrum of SSP PEDOT matches well with the PH1000 spectrum, indicating they are nearly identical polymers. More specifically, the peaks at 438 cm^{-1}, 575 cm^{-1}, and 988 cm^{-1} are associated with the deformation of oxyethylene ring (Shi et al., 2017). The peaks at 696 cm^{-1}, 853 cm^{-1}, and 1,103 cm^{-1} are in connection with symmetric C-S-C and C-O-C stretching (Shi et al., 2017). The bands at 1,262 cm^{-1}, 1,364 cm^{-1}, and 1,427 cm^{-1} (1,441 cm^{-1} in PH1000) correspond to the C_α-C_α, C_β-C_β, and symmetric $C_\alpha = C_\beta$ stretching vibrations, respectively (see Figure 1C for assignment of $C_\alpha$and C_β) (Hofmann et al., 2017). These characteristic resonance peaks reflect the structure of a PEDOT chain (Shi et al., 2017; Ouyang et al., 2005). The FTIR and Raman spectra together suggest that the PEDOT is synthesized successfully by the sequential solution polymerization method.

Compositional Analysis of SSP PEDOT Film

The as-cast film usually contains undesirable excess EDOT monomers, oxidants, and the reduced oxidants, which could physically incorporate in the polymer matrix and influence the film properties (Ouyang et al.,

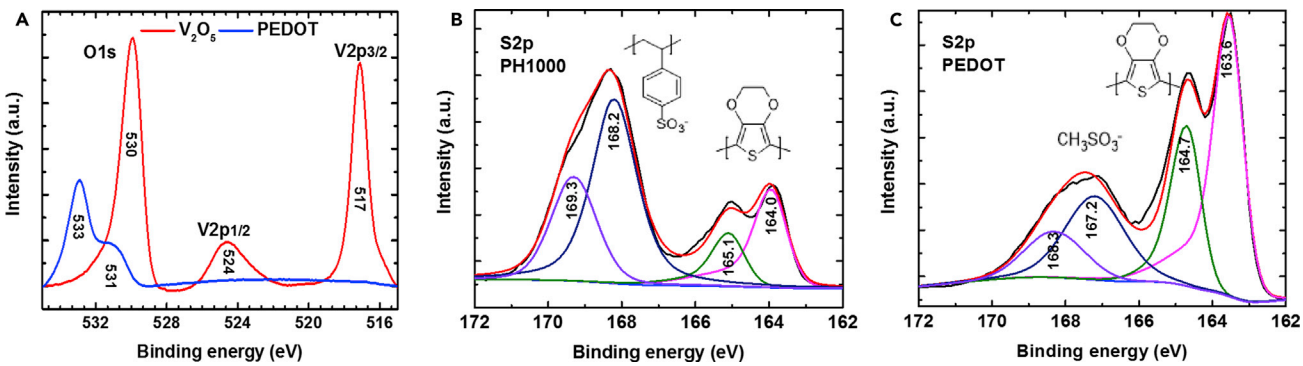

Figure 2. Compositional Analysis of SSP PEDOT Film

(A) XPS spectra (V2p) of V_2O_5 and SSP PEDOT.

(B) XPS spectra (S2p) of PH1000.

(C) XPS spectra (S2p) of SSP PEDOT.

2018). So rinsing the as-cast film is necessary. In FTIR spectra, the =C-H deformation vibrations were absent from SSP PEDOT, showing that the excess EDOT monomers can be removed by MeOH rinsing. A more detailed compositional analysis is carried out with X-ray photoelectron spectroscopy (XPS). As presented in Figure 2A, V_2O_5 exhibits three typical peaks in the binding energy between 515 and 535 eV. The peak centered at 530 eV comes from the O1s core level (Tehrani et al., 2007; Guo et al., 2014; Ohno et al., 2001). The other two peaks positioned at 517 and 524 eV are from the $V2p_{3/2}$ and $V2p_{1/2}$ orbitals, respectively (Li et al., 2018). Interestingly, the V2p signals completely disappear in SSP PEDOT, which means no oxidant residue is left in the PEDOT film. An observable change has happened to the O1s peak. The band around 533 eV can be attributed to the C-O bond in PEDOT, whereas the peak at 531 eV can be assigned to S=O in the counterions (Madl et al., 2011; Kim et al., 2009; Park et al., 2014; Yan and Okuzaki, 2009). It can be concluded from the XPS and FTIR analyses that the MeOH-rinsed film contains only PEDOT and its counterions without residual reactants or oxidants.

To figure out the concentration of counterions in the SSP PEDOT film, XPS fine scan on S2p was carried out and compared with PH1000 (Figures 2B and 2C). The S2p electrons associated with each moiety possess different binding energies owing to their different chemical environments. For example, the doublet peaks between 162 and 167 eV are related to the sulfur atoms in the PEDOT, whereas the band from 167 to 172 eV comes from the sulfonate groups in the counterions, i.e., MSA or PSS (Sarker et al., 2015; Wu et al., 2017; Rudd et al., 2018). The area ratio of the two bands could be used to estimate the relative molar ratio of PEDOT and counterions in the film. For the PH1000 sample, the relative molar ratio of PEDOT to PSS is close to 1:2, which is consistent with the weight ratio of 1:2.5 provided by Heraeus (Takano et al., 2012; Xia and Ouyang, 2010; Lipomi et al., 2012). The small PEDOT/PSS ratio indicates that a large number of insulating PSS exist in the PH1000 film. In great contrast, the ratio between PEDOT and MSA in SSP PEDOT film is much higher, up to 2.2:1. This result demonstrates that PEDOT is the dominant component in the SSP PEDOT film.

Electrical Properties of SSP PEDOT Film

The electrical properties of PH1000 and synthesized PEDOT are summarized and listed in Table 1. The electrical conductivity of synthesized PEDOT film can reach 1,420 S/cm, with an average value around 1,333 S/cm, whereas the conductivity of PH1000 is lower than 0.5 S/cm. As the conductivity (σ) is related to carrier concentration (p) and carrier mobility (μ), $\sigma = qp\mu$ (q is the unit charge, 1.6×10^{-19} C) (Lee et al., 2014), Hall effect measurement is carried out to pinpoint the change in p or μ or both. The average Hall mobilities of SSP PEDOT and PH1000 are 2.70 cm^2/Vs and 2.41 cm^2/Vs, respectively, which are quite comparable. However, the carrier concentration of SSP PEDOT (2.62^{21} cm^{-3}) is three orders of magnitude higher than that of PH1000 (2.60^{18} cm^{-3}). So the high conductivity of SSP PEDOT is mainly due to the high carrier concentration.

Oxidation State of SSP PEDOT Film

The carrier concentration has a direct correlation with the doping level of PEDOT chains. To learn about the oxidative state of SSP PEDOT, ultraviolet-visible-near-infrared (UV-vis-NIR) absorption spectra of SSP

Sample	Sheet Resistance[a,b] Ω/sq	Conductivity[a] (S/cm)	Carrier Concentration[c] (cm^{-3})	Carrier Mobility[c] (cm^2/Vs)
PH1000	(303 ± 24) × 10^3	0.43±0.04	(2.60 ± 0.84)×10^{18}	2.41±0.93
SSP PEDOT	103.10 ± 10.37	1,333.59±86.28	(2.62 ± 0.74)×10^{21}	2.70±0.73

Table 1. Electrical Properties of SSP PEDOT Film

Data are represented as mean ± SEM.

[a]Measured by the four-point probe (van der Pauw) method.

[b]The film thickness of PH1000 and SSP PEDOT were ~70 nm.

[c]Measured by Hall effect system.

PEDOT and PH1000 films were recorded. According to the literatures (Cutler et al., 2002; Hyeonseok and Jyongsik, 2009; Ouyang et al., 2018; Park et al., 2014), the absorption band around 600 nm is attributed to $\pi \rightarrow \pi^*$ transition of the thiophene rings at neutral state; it will shift to 800 and 1,200 nm after being oxidized to the polaron and bipolaron states, respectively. The UV-vis-NIR spectra of synthesized PEDOT and PH1000 normalized with film thickness are displayed in Figure 3A. From 400 to 1,200 nm, the normalized absorption spectrum of SSP PEDOT exhibits a stronger intensity than that of PH1000, implying that the carrier concentration in all three states is higher than that of PH1000. SSP PEDOT shows a strong absorption band at 900 nm, suggesting that the polaron state is dominant in SSP PEDOT.

To further understand the oxidation state of the PEDOT chains, the main Raman peaks of SSP PEDOT and PH1000 are deconvoluted and compared (Figures 3B and 3C). The most notable peak at 1,427 cm^{-1} in Figure 3B and at 1,441 cm^{-1} in Figure 3C correspond to the symmetric C=C stretching vibration in the thiophene rings of PEDOT (Ji et al., 2015). This peak is a combination of two bands, one at a smaller Raman shift is due to the vibration of the benzoid (neutral) structure and the other one at a slightly higher Raman shift is related to the quinoid (oxidized) structure (see Figure 1C for the benzoid or quinoid structures) (Wu et al., 2017; Chiu et al., 2005, 2006; Hyeonseok and Jyongsik, 2009). So the area ratio of the two peaks (oxidized/neutral) reflects the doping level of PEDOT chains to some extent. Following this calculation, the ratio between quinoid and benzoid structures in SSP PEDOT is close to 0.35, whereas that of the PH1000 film is only 0.20. The oxidized chains in SSP PEDOT are much more than that in PH1000, reflecting a higher doping level (Ouyang et al., 2005). This explains why SSP PEDOT possesses higher carrier concentration.

The Molecular Packing of SSP PEDOT

The molecular packing in nano- and microscale is of importance to carrier transport. Atomic force microscopy is employed to compare the surface morphology of the SPP PEDOT film with that of the PH1000 film. As shown in Figure 4A, the average grain size of the PH1000 film is small and the surface of the film is smooth with a root-mean-square roughness (Rq) of 1.44 nm. In contrast, a much larger domain size and rougher surface are observed in Figure 4B, with a Rq of 11.28 nm. It was reported that rinsing the as-cast PEDOT films could cause a collapse and volume contraction of the film due to removal of residuals (Ouyang et al., 2018; Winther-Jensen et al., 2005). Owing to this, SSP PEDOT displays a more aggregated yet slightly rougher surface (Mayevsky et al., 2016).

Figure 4C shows the particle size distribution of the SSP PEDOT and PH1000 dispersed in deionized (DI) water by ultrasonication for 3 min. The average particle size of the SSP PEDOT is 348.65 μm, which is much higher than that of the PH1000 (1.84 μm). The average particle size is an indicator of the molecular size of the polymers (Zhang et al., 2016), as well as inter-chain interactions (Bahry et al., 2018). Therefore, a larger average particle size is expected to provide better charge transport due to longer conjugation length and easier charge hopping between adjacent backbones (Wang et al., 2013).

To further confirm that the inter-chain interaction plays a role in the aggregation, X-ray diffraction (XRD) patterns of SSP PEDOT and pristine PH1000 film are recorded (Figure 4D). Both spectra exhibit a broad peak in the range of 15°–35°, which is due to the glass substrate (Lee et al., 2014). For the PH1000 sample, only the broad peak centered at 23° could be observed, indicating that the polymers are completely amorphous without any crystallinity (Raghava et al., 2010; Illakkiya et al., 2018; Kim et al., 2014; Bahry et al., 2018; Ma et al., 2005). In great contrast, a sharp peak centered at 24.8° emerged in the diffraction pattern of SSP

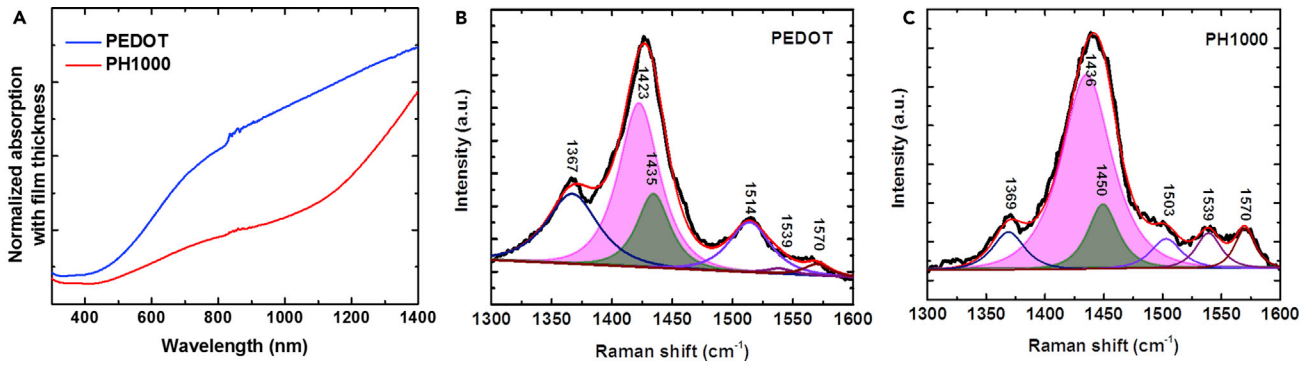

Figure 3. Oxidation state of SSP PEDOT Film

(A) UV-vis-NIR absorption spectra of SSP PEDOT and PH1000 normalized with film thickness.

(B and C) Deconvolution Raman spectra for SSP PEDOT (B) and PH1000 (C) in the range of 1,300–1,600 cm^{-1}.

PEDOT, followed by a lower peak at 50.6°. These two peaks resemble the first- and second-order diffraction peaks, suggesting the existence of crystal region. The first peak corresponds to a d-spacing of 3.6 Å, which is close to the typical π-π stacking distance, signifying that some PEDOT chains in SSP PEDOT have a well-ordered π-π stacking (Kumar et al., 2016; Sun et al., 2015b; Chen et al., 2017; Wang et al., 2018b; Rudd et al., 2018). However, the result cannot rule out the possibility that the crystalline PEDOT domains could be embedded in an amorphous PEDOT matrix (Rolland et al., 2018; Gueye et al., 2016). The mean crystal size derived using Scherrer equation is 42.8 nm. The XRD results confirm that SSP PEDOT exhibits a high crystallinity that is beneficial for charge transport.

Large-Scale Polymerization and Realization of Flexible Touch Screen

The synthetic route can be easily transferred to large-scale fabrication. Here we demonstrate printing of 15 × 12 cm PEDOT films on PET by bar coating. In brief, the oxidant solution is first bar coated on a PET

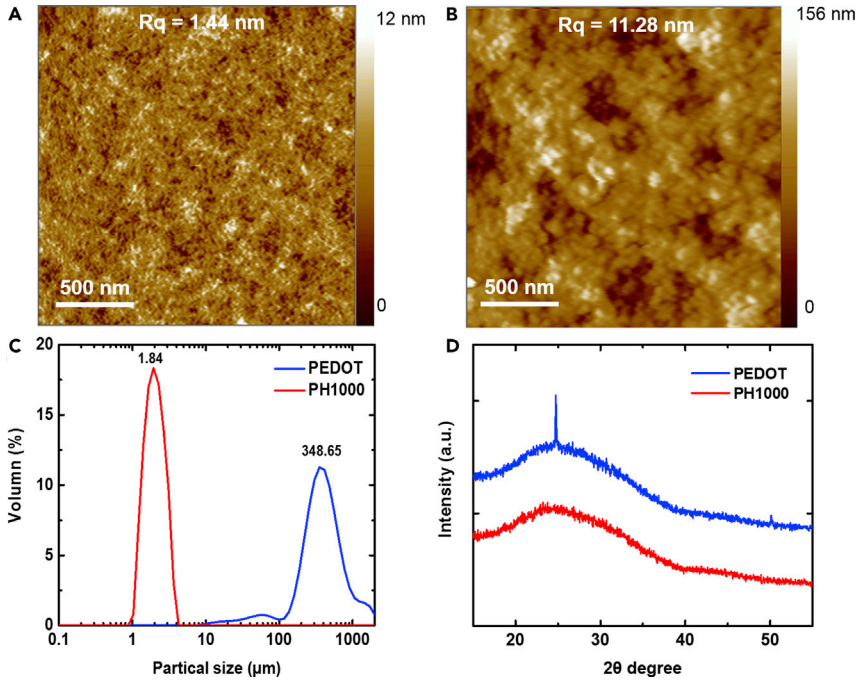

Figure 4. The Molecular Packing of SSP PEDOT

(A and B) Atomic force microscopic height images of PH1000 and SSP PEDOT; the image size is 2 × 2 μm.

(C) Particle size distribution of SSP PEDOT and PH1000.

(D) XRD spectra of SSP PEDOT and PH1000.

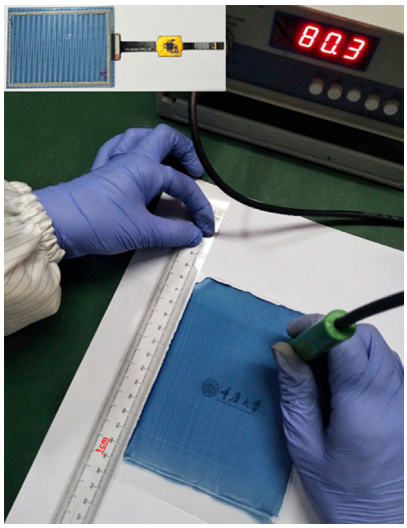

Figure 5. Large-Scale Polymerization and Realization of Flexible Touch Screen

The photograph of the SSP PEDOT film synthesized on a 15 × 12 cm PET substrate by sequential solution polymerization with a sheet resistance of 80.3 Ω/sq; see also Video S1.

The inset is a 2-in touch sensor made by the SSP PEDOT film; see also Videos S2 and S3.

substrate, which is quickly immersed in the monomer solution where PEDOT film forms in less than 1 s. The whole process is displayed in Video S1. It is believed that this synthetic route can be further adaptable to other solution-based manufacturing techniques, such as doctor blading, screen printing, inkjet printing, or roll-to-roll printing, etc. As shown in Figure 5, the obtained PEDOT film is homogeneous with a sheet resistance of 80.3 Ω sq^{-1}, which is low enough for many applications such as electromagnetic shielding, antistatic coatings, and sensors.

Owing to the low sheet resistance and high flexibility, the SSP PEDOT film is used to fabricate capacitive touch sensors (see inset of Figure 5). When connected to a controller and a computer, the sensor allows humans to input information by touching the surface. Touch functions of the sensor are shown in Video S2. We demonstrated writing the abbreviation of Chongqing University (CQU) on the touch sensor. We further showed that the flexible touch sensor could maintain its touch functions after bending back and forth, or even being folded at a bending radius less than 1 mm. The extremely high flexibility of the touch sensor will provide more interfaces for human-machine interactions (Wang et al., 2018a; Pu et al., 2017; Kim et al., 2018). Besides the ultrahigh flexibility, the touch sensors made from SSP PEDOT also exhibit high sensitivity. As demonstrated in Video S3, the sensor is able to control the rotation of a motor or the brightness of a light bulb even if it is beneath a piece of leather. Such a combination with leathers can lead to many new opportunities in control applications, such as in smart homes and automobiles.

Conclusion

A low-cost and high-throughput synthetic route for PEDOT films is highly desirable because of the wide applications of the transparent and conducting polymer films. In this work, a novel and facial method is introduced to fabricate highly conductive PEDOT films *in situ* by solution means. The process consists of sequential solution deposition of oxidants and monomers and can be completed within a minute. The subsequent MeOH rinsing can effectively remove excess EDOT monomers and oxidants in the synthesized PEDOT films. Characterization shows that PEDOT is the dominant component in the film that is heavily doped by the MSA counterions. The SSP PEDOT possesses good crystallinity, extremely high carrier concentration, and good carrier mobility, all of which contribute to its high electrical conductivity, which reaches 1,420 S/cm. We further demonstrate that the synthesis method can be extended to large-scale printing techniques on flexible substrate. The printed films exhibit a sheet resistance of 81 Ω sq^{-1}, which is low enough for many applications. For demonstration, flexible capacitive touch sensors are made from the SSP PEDOT film. The sensors exhibit superior flexibility and ultrahigh sensitivity. The results together suggest that sequential solution polymerization is a scalable new method that is ideal for the industrial production of conjugated polymer films.

Limitations of the Study

In this work, a novel synthetic route is demonstrated to polymerize PEDOT *in situ* on both glass and PET substrates. Although the conducting polymer film exhibits high conductivity, excellent flexibility, and

good stability, the optical transparency is still not ideal. Future investigations will seek to improve its optical properties. Furthermore, it is necessary to demonstrate that the new method is applicable to other conducting polymers.

METHODS

All methods can be found in the accompanying Transparent Methods supplemental file.

SUPPLEMENTAL INFORMATION

Supplemental Information includes Transparent Methods and three videos and can be found with this article online at https://doi.org/10.1016/j.isci.2019.01.003.

ACKNOWLEDGMENTS

This work was financially supported by research grants from the Natural Science Foundation of China (61504015, 51702032), the Natural Science Foundation of Chongqing (cstc2017jcyjAX0451, cstc2017rgzn-zdyfX0023, cstc2018jszx-cyzd0603), the Key Laboratory of Low-grade Energy Utilization Technologies and Systems (LLEUTS-2017004), Venture & Innovation Support Program for Chongqing Overseas Returnees (cx2017034, cx2017056), and Fundamental Research Funds for the Central Universities (106112017CDJQJ148805, 2018CDQYDL0051).

AUTHOR CONTRIBUTIONS

R.C. polymerized the PEDOT film and characterized the film properties using VDP, Hall effect, FTIR, Raman, XPS, UV-vis-NIR, AFM, and XRD. Y.W. and X.L. performed DLS characterization and analysis. Q.Z. and Y.Z. scaled up the synthesis to print the large-area PEDOT films. J.X., C.M., and Y.Z. fabricated the flexible touch screen sensors and touch leathers. Y.S. and Z.W. made the program to use touch leathers to control motor and light bulb. K.S. and J.O. conceived the idea. R.C. and M.L. prepared the manuscript. K.S. and J.O. supervised the project and revised the manuscript. All authors discussed the results and commented on the manuscript.

DECLARATION OF INTERESTS

PCT and Chinese patents have been filed for the technology described in the article.

Received: September 30, 2018
Revised: December 11, 2018
Accepted: January 2, 2019
Published: February 22, 2019

REFERENCES

Alf, M.E., Asatekin, A., Barr, M.C., Baxamusa, S.H., Chelawat, H., Ozaydin-Ince, G., Petruczok, C.D., Sreenivasan, R., Tenhaeff, W.E., Trujillo, N.J., et al. (2010). Chemical vapor deposition of conformal, functional, and responsive polymer films. Adv. Mater. *22*, 1993–2027.

Bahry, T., Cui, Z.P., Deniset-Besseau, A., Gervais, M., Sollogoub, C., Bui, T.T., and Remita, S. (2018). An alternative radiolytic route for synthesizing conducting polymers in an organic solvent. New J. Chem. *42*, 8704–8716.

Bashir, T., Bakare, F., Baghaei, B., Mehrjerdi, A.K., and Skrifvars, M. (2013). Influence of different organic solvents and oxidants on insulating and film-forming properties of PEDOT polymer. Iran. Polym. J. *22*, 599–611.

Benoit, R.L., Frechette, M., and Lefebvre, D. (1988). 2,6-Di-Tert-Butylpyridine - an unusually weak base in dimethylsulfoxide. Can. J. Chem. Rev. Can. Chim. *66*, 1159–1162.

Bhattacharyya, D., Howden, R.M., Borrelli, D.C., and Gleason, K.K. (2012). Vapor phase oxidative synthesis of conjugated polymers and applications. J. Polym. Sci. B Polym. Phys. *50*, 1329–1351.

Chen, Q., Chen, L., Ye, F., Zhao, T., Tang, F., Rajagopal, A., Jiang, Z., Jiang, S., Jen, A.K., Xie, Y., et al. (2017). Ag-incorporated organic-inorganic perovskite films and planar heterojunction solar cells. Nano Lett. *17*, 3231–3237.

Chiu, W.W., Travas-Sejdic, J., Cooney, R.P., and Bowmaker, G.A. (2005). Spectroscopic and conductivity studies of doping in chemically synthesized poly(3,4-ethylenedioxythiophene). Synth. Met. *155*, 80–88.

Chiu, W.W., Travaš-Sejdić, J., Cooney, R.P., and Bowmaker, G.A. (2006). Studies of dopant effects in poly(3,4-ethylenedi-oxythiophene) using Raman spectroscopy. J. Raman Spectrosc. *37*, 1354–1361.

Cho, B., Park, K.S., Baek, J., Oh, H.S., Koo Lee, Y.E., and Sung, M.M. (2014). Single-crystal poly(3,4-ethylenedioxythiophene) nanowires with ultrahigh conductivity. Nano Lett. *14*, 3321–3327.

Coletta, C., Cui, Z.P., Dazzi, A., Guigner, J.M., Neron, S., Marignier, J.L., and Remita, S. (2016). A pulsed electron beam synthesis of PEDOT conducting polymers by using sulfate radicals as oxidizing species. Radiat. Phys. Chem. *126*, 21–31.

Cutler, C.A., Bouguettaya, M., and Reynolds, J.R. (2002). PEDOT polyelectrolyte based electrochromic films via electrostatic adsorption. Adv. Mater. *14*, 684–688.

Dong, Q.F., Zhou, Y.H., Pei, J.N., Liu, Z.Y., Li, Y.W., Yao, S.Y., Zhang, J.B., and Tian, W.J. (2010). All-spin-coating vacuum-free processed semi-transparent inverted polymer solar cells with

PEDOT: PSS anode and PAH-D interfacial layer. Org. Electron. *11*, 1327–1331.

Fabretto, M., Zuber, K., Hall, C., Murphy, P., and Griesser, H.J. (2009). The role of water in the synthesis and performance of vapour phase polymerised PEDOT electrochromic devices. J. Mater. Chem. *19*, 7871–7878.

Fabretto, M.V., Evans, D.R., Mueller, M., Zuber, K., Hojati-Talemi, P., Short, R.D., Wallace, G.G., and Murphy, P.J. (2012). Polymeric material with metal-like conductivity for next generation organic electronic devices. Chem. Mater. *24*, 3998–4003.

Ghosh, S., Remita, H., Ramos, L., Dazzi, A., Deniset-Besseau, A., Beaunier, P., Goubard, F., Aubert, P.H., Brisset, F., and Remita, S. (2014). PEDOT nanostructures synthesized in hexagonal mesophases. New J. Chem. *38*, 1106–1115.

Gueye, M.N., Carella, A., Massonnet, N., Yvenou, E., Brenet, S., Faure-Vincent, J., Pouget, S., Rieutord, F., Okuno, H., Benayad, A., et al. (2016). Structure and dopant engineering in PEDOT thin films: practical tools for a dramatic conductivity enhancement. Chem. Mater. *28*, 3462–3468.

Guo, C.X., Sun, K., Ouyang, J.Y., and Lu, X.M. (2015a). Layered V2O5/PEDOT nanowires and ultrathin nanobelts fabricated with a silk reelinglike process. Chem. Mater. *27*, 5813–5819.

Guo, C.X., Yilmaz, G., Chen, S.C., Chen, S.F., and Lu, X.M. (2015b). Hierarchical nanocomposite composed of layered V2O5/PEDOT/MnO2 nanosheets for high-performance asymmetric supercapacitors. Nano Energy *12*, 76–87.

Guo, Y.X., Zou, C.W., Liu, Y.F., Xu, Y.Q., Wang, X.L., Yu, J.Y., Yang, Z.Y., Zhang, F., and Zhou, R. (2014). Facile preparation of vanadium oxide thin films on sapphire(0001) by sol–gel method. J. Sol Gel Sci. Technol. *70*, 40–46.

Hofmann, A.I., Katsigiannopoulos, D., Mumtaz, M., Petsagkourakis, I., Pecastaings, G., Fleury, G., Schatz, C., Pavlopoulou, E., Brochon, C., Hadziioannou, G., and Cloutet, E. (2017). How to choose polyelectrolytes for aqueous dispersions of conducting PEDOT complexes. Macromolecules *50*, 1959–1969.

Huang, J.H., and Chu, C.W. (2011). Achieving efficient poly(3,4-ethylenedioxythiophene)-based supercapacitors by controlling the polymerization kinetics. Electrochim. Acta *56*, 7228–7234.

Hyeonseok, Y., and Jyongsik, J. (2009). Conducting-polymer nanomaterials for high-performance sensor applications: issues and challenges. Adv. Funct. Mater. *19*, 1567–1576.

Illakkiya, J.T., Rajalakshmi, P.U., and Oommen, R. (2018). Synthesis and characterization of transparent conducting SWCNT/PEDOT: PSS composite films by spin coating technique. Optik *157*, 435–440.

Ji, T., Tan, L., Hu, X., Dai, Y., and Chen, Y. (2015). A comprehensive study of sulfonated carbon materials as conductive composites for polymer solar cells. Phys. Chem. Chem. Phys. *17*, 4137–4145.

Kim, J., Kim, E., Won, Y., Lee, H., and Suh, K. (2003). The preparation and characteristics of conductive poly(3,4-ethylenedioxythiophene) thin film by vapor-phase polymerization. Synth. Met. *139*, 485–489.

Kim, N., Kee, S., Lee, S.H., Lee, B.H., Kahng, Y.H., Jo, Y.R., Kim, B.J., and Lee, K. (2014). Highly conductive PEDOT: PSS nanofibrils induced by solution-processed crystallization. Adv. Mater. *26*, 2268–2272.

Kim, T.W., Woo, H.Y., Jung, W.G., Ihm, D.W., and Kim, J.Y. (2009). On the mechanism of conductivity enhancement in plasma treated poly(3,4-ethylenedioxythiophene) films. Thin Solid Films *517*, 4147–4151.

Kim, Y., Chortos, A., Xu, W., Liu, Y., Oh, J.Y., Son, D., Kang, J., Foudeh, A.M., Zhu, C., Lee, Y., et al. (2018). A bioinspired flexible organic artificial afferent nerve. Science *360*, 998–1003.

Kumar, P.N., Kolay, A., Kumar, S.K., Patra, P., Aphale, A., Srivastava, A.K., and Deepa, M. (2016). Counter electrode impact on quantum dot solar cell efficiencies. ACS Appl. Mater. Interfaces *8*, 27688–27700.

Lee, S., Paine, D.C., and Gleason, K.K. (2014). Heavily doped poly(3,4-ethylenedioxythiophene) thin films with high carrier mobility deposited using oxidative CVD: conductivity stability and carrier transport. Adv. Funct. Mater. *24*, 7187–7196.

Lee, S.H., and Gleason, K.K. (2015). Enhanced optical property with tunable band gap of cross-linked PEDOT copolymers via oxidative chemical vapor deposition. Adv. Funct. Mater. *25*, 85–93.

Li, J.X., and Ma, Y.X. (2016). In-situ synthesis of transparent conductive PEDOT coating on PET foil by liquid phase depositional polymerization of EDOT. Synth. Met. *217*, 185–188.

Li, Y.B., Liu, J.C., Wang, D.P., Pan, G.Y., and Dang, Y.Y. (2018). Effects of the annealing process on the structure and valence state of vanadium oxide thin films. Mater. Res. Bull. *100*, 220–225.

Lipomi, D.J., Lee, J.A., Vosgueritchian, M., Tee, B.C.K., Bolander, J.A., and Bao, Z.A. (2012). Electronic properties of transparent conductive films of PEDOT: PSS on stretchable substrates. Chem. Mater. *24*, 373–382.

Loganathan, K., and Pickup, P.G. (2005). Poly(Δ4,4′-dicyclopenta[2,1-b:3,4-b′] dithiophene–co-3,4-ethylenedioxythiophene): Electrochemically generated low band gap conducting copolymers. Electrochim. Acta *51*, 41–46.

Ma, W.L., Yang, C.Y., Gong, X., Lee, K., and Heeger, A.J. (2005). Thermally stable, efficient polymer solar cells with nanoscale control of the interpenetrating network morphology. Adv. Funct. Mater. *15*, 1617–1622.

Madl, C.M., Kariuki, P.N., Gendron, J., Piper, L.F.J., and Jones, W.E. (2011). Vapor phase polymerization of poly (3,4-ethylenedioxythiophene) on flexible substrates for enhanced transparent electrodes. Synth. Met. *161*, 1159–1165.

Mayevsky, D., Gann, E., Garvey, C.J., Mcneill, C.R., and Winther-Jensen, B. (2016). Decoupling order and conductivity in doped conducting polymers. Phys. Chem. Chem. Phys. *18*, 19397–19404.

Metsik, J., Saal, K., Maeorg, U., Lohmus, R., Leinberg, S., Mandar, H., Kodu, M., and Timusk, M. (2014). Growth of poly(3,4-ethylenedioxythiophene)films prepared by base-inhibited vapor phase polymerization. J. Polym. Sci. B Polym. Phys. *52*, 561–571.

Murugan, A.V., Kale, B.B., Kwon, C.-W., Campet, G., and Vijayamohanan, K. (2001). Synthesis and characterization of a new organo–inorganic poly(3,4-ethylene dioxythiophene) PEDOT/V2O5 nanocomposite by intercalation. J. Mater. Chem. *11*, 2470–2475.

Ohno, T., Masaki, Y., Hirayama, S., and Matsumura, M. (2001). TiO2-photocatalyzed epoxidation of 1-decene by H2O2 under visible light. J. Catal. *204*, 163–168.

Ouyang, J., Chu, C., Chen, F., Xu, Q., and Yang, Y. (2005). High-conductivity poly (3, 4-ethylenedioxythiophene)-poly (styrene sulfonate) film and its application in polymer optoelectronic devices. Adv. Funct. Mater. *15*, 203–208.

Ouyang, L.Q., Jafari, M.J., Cai, W.Z., Aguirre, L.E., Wang, C.F., Ederth, T., and Inganas, O. (2018). The contraction of PEDOT films formed on a macromolecular liquid-like surface. J. Mater. Chem. C *6*, 654–660.

Park, H., Lee, S.H., Kim, F.S., Choi, H.H., Cheong, I.W., and Kim, J.H. (2014). Enhanced thermoelectric properties of PEDOT: PSS nanofilms by a chemical dedoping process. J. Mater. Chem. A *2*, 6532–6539.

Pu, X., Guo, H., Chen, J., Wang, X., Xi, Y., Hu, C., and Wang, Z.L. (2017). Eye motion triggered self-powered mechnosensational communication system using triboelectricnanogenerator. Sci. Adv. *3*, e1700694.

Raghava, R.K., Mo, J.H., Youngil, L., and Venkataramanaiah, R.A. (2010). Synthesis of MWCNTs-core/thiophene polymer-sheath composite nanocables by a cationic surfactant-assisted chemical oxidative polymerization and their structural properties. J. Polym. Sci. A Polym. Chem. *48*, 1477–1484.

Rolland, N., Franco-Gonzalez, J.F., Volpi, R., Linares, M., and Zozoulenko, I.V. (2018). Understanding morphology-mobility dependence in PEDOT: Tos. Phys. Rev. Mater. *2*, 045605.

Rudd, S., Franco-Gonzalez, J.F., Kumar Singh, S., Ullah Khan, Z., Crispin, X., Andreasen, J.W., Zozoulenko, I., and Evans, D. (2018). Charge transport and structure in semimetallic polymers. J. Polym. Sci. B Polym. Phys. *56*, 97–104.

Sarker, A.K., Kim, J., Wee, B.H., Song, H.J., Lee, Y., Hong, J.D., and Lee, C. (2015). Hydroiodic acid treated PEDOT: PSS thin film as transparent electrode: an approach towards ITO free organic photovoltaics. RSC Adv. *5*, 52019–52025.

Schoetz, T., Ponce De Leon, C., Bund, A., and Ueda, M. (2018). Electro-polymerisation and characterisation of PEDOT in Lewis basic, neutral and acidic EMImCl-AlCl 3 ionic liquid. Electrochim. Acta *263*, 176–183.

Shi, W., Yao, Q., Qu, S.Y., Chen, H.Y., Zhang, T.S., and Chen, L.D. (2017). Micron-thick highly conductive PEDOT films synthesized via self-inhibited polymerization: roles of anions. NPG Asia Mater. *9*, e405.

Sun, K., Li, P., Xia, Y., Chang, J., and Ouyang, J. (2015a). Transparent conductive oxide-free perovskite solar cells with PEDOT: PSS as transparent electrode. ACS Appl. Mater. Interfaces *7*, 15314–15320.

Sun, K., Xiao, Z., Lu, S., Zajaczkowski, W., Pisula, W., Hanssen, E., White, J.M., Williamson, R.M., Subbiah, J., Ouyang, J., et al. (2015b). A molecular nematic liquid crystalline material for high-performance organic photovoltaics. Nat. Commun. *6*, 6013.

Sun, K., Zhang, S.P., Li, P.C., Xia, Y.J., Zhang, X., Du, D.H., Isikgor, F.H., and Ouyang, J.Y. (2015c). Review on application of PEDOTs and PEDOT: PSS in energy conversion and storage devices. J. Mater. Sci. Mater. Electron. *26*, 4438–4462.

Syed ZainolAbidin, S.N.J., Mamat, M.S., Rasyid, S.A., Zainal, Z., and Sulaiman, Y. (2018). Electropolymerization of poly(3,4-ethylenedioxythiophene) onto polyvinyl alcohol-graphene quantum dot-cobalt oxide nanofiber composite for high-performance supercapacitor. Electrochim. Acta *261*, 548–556.

Takano, T., Masunaga, H., Fujiwara, A., Okuzaki, H., and Sasaki, T. (2012). PEDOT nanocrystal in highly conductive PEDOT: PSS polymer films. Macromolecules *45*, 3859–3865.

Tehrani, P., Kanciurzewska, A., Crispin, X., Robinson, N.D., Fahlman, M., and Berggren, M. (2007). The effect of pH on the electrochemical over-oxidation in PEDOT : PSS films. Solid State Ionics *177*, 3521–3527.

Vaillant, J., Lira-Cantu, M., Cuentas-Gallegos, K., Casan-Pastor, N., and Gomez-Romero, P. (2006). Chemical synthesis of hybrid materials based on PAni and PEDOT with polyoxometalates for electrochemical supercapacitors. Prog. Solid State Chem. *34*, 147–159.

Wang, H.Y., Xu, Y.Z., Yu, X.H., Xing, R.B., Liu, J.G., and Han, Y.C. (2013). Structure and morphology control in thin films of conjugated polymers for an improved charge transport. Polymers *5*, 1272–1324.

Wang, S., Xu, J., Wang, W., Wang, G.N., Rastak, R., Molina-Lopez, F., Chung, J.W., Niu, S., Feig, V.R., Lopez, J., et al. (2018a). Skin electronics from scalable fabrication of an intrinsically stretchable transistor array. Nature *555*, 83–88.

Wang, X., Zhang, X., Sun, L., Lee, D., Lee, S., Wang, M., Zhao, J., Shao-Horn, Y., Dinca, M., Palacios, T., and Gleason, K.K. (2018b). High electrical conductivity and carrier mobility in oCVD PEDOT thin films by engineered crystallization and acid treatment. Sci. Adv. *4*, eaat5780.

Winther-Jensen, B., Chen, J., West, K., and Wallace, G. (2005). 'Stuffed' conducting polymers. Polymer *46*, 4664–4669.

Winther-Jensen, B., and West, K. (2004). Vapor-phase polymerization of 3,4-ethylenedioxythiophene- a route to highly conducting polymer surface layers. Macromolecules *37*, 4538–4543.

Wu, F.L., Li, P.C., Sun, K.A., Zhou, Y.L., Chen, W., Fu, J.H., Li, M., Lu, S.R., Wei, D.S., Tang, X.S., et al. (2017). Conductivity enhancement of PEDOT: PSS via addition of chloroplatinic acid and its mechanism. Adv. Electron. Mater. *3*, 1700047.

Xia, Y., Fang, J., Li, P., Zhang, B., Yao, H., Chen, J., Ding, J., and Ouyang, J. (2017). Solution-processed highly superparamagnetic and conductive PEDOT: PSS/Fe3O4 nanocomposite films with high transparency and high mechanical flexibility. ACS Appl. Mater. Interfaces *9*, 19001–19010.

Xia, Y.J., and Ouyang, J.Y. (2010). Anion effect on salt-induced conductivity enhancement of poly(3,4-ethylenedioxythiophene):poly(styrenesulfonate) films. Org. Electron. *11*, 1129–1135.

Yan, H., and Okuzaki, H. (2009). Effect of solvent on PEDOT/PSS nanometer-scaled thin films: XPS and STEM/AFM studies. Synth. Met. *159*, 2225–2228.

Zhang, S.P., Yu, Z.M., Li, P.C., Li, B.C., Isikgor, F.H., Du, D.H., Sun, K., Xia, Y.J., and Ouyang, J.Y. (2016). Poly(3,4-ethylenedioxythiophene):polystyrene sulfonate films with low conductivity and low acidity through a treatment of their solutions with probe ultrasonication and their application as hole transport layer in polymer solar cells and perovskite solar cells. Org. Electron. *32*, 149–156.

Zhang, X., Macdiarmid, A.G., and Manohar, S.K. (2005). Chemical synthesis of PEDOT nanofibers. Chem. Commun. (Camb.) *42*, 5328–5330.

Zhou, Y.H., Cheun, H., Choi, S., Potscavage, W.J., Fuentes-Hernandez, C., and Kippelen, B. (2010). Indium tin oxide-free and metal-free semitransparent organic solar cells. Appl. Phys. Lett. *97*, 153304.

Zuber, K., Fabretto, M., Hall, C., and Murphy, P. (2008). Improved PEDOT conductivity via suppression of crystallite formation in Fe(III) tosylate during vapor phase polymerization. Macromol. Rapid Commun. *29*, 1503–1508.

ISCI, Volume *12*

Supplemental Information

Sequential Solution Polymerization of Poly(3,4-ethylenedioxythiophene) Using V_2O_5 as Oxidant for Flexible Touch Sensors

Rui Chen, Kuan Sun, Qi Zhang, Yongli Zhou, Meng Li, Yuyang Sun, Zhou Wu, Yuyang Wu, Xinlu Li, Jialei Xi, Chi Ma, Yiyang Zhang, and Jianyong Ouyang

Transparent Methods

1. Materials

3,4-Ethylenedioxythiophene (EDOT, P1328908, 99%), 2,6-di-tert-butylpyridine (DTBP, P1216954, 98%) and methanesulfonic acid (MSA, P1306518, 99%) were obtained from Adamas Reagent. Acetonitrile (MeCN, 80988I, 99%), vanadium pentoxide (V_2O_5, 20150613, 99%), methanol (MeOH, 2016012901, 99.5%), Triton X-100 (P1128113, 98%), petroleum ether (P1190274, 99%) and dimethyl sulfoxide (DMSO, 2015060801, 99%) were purchased from Sinopharm Chemica. All reagents were used without further purification.

2. Sequential Solution Polymerize PEDOT on Glass by Spin-Coating

To obtain the oxidant precursor, 0.45 g V_2O_5 was added in 12 mL MSA, sealed in a volumetric flask, stirred for 24 hrs with a magnetic stirrer and then aged for a month. The oxidant solution was formed taking the supernatant and blended with DTBP at a volume ratio of 475 : 575. The monomer solution was a mixture of EDOT and acetonitrile at a volume ratio of 9 : 1. The oxidant solution was spin-cast at 3000 r.p.m. for 12 s onto a 15 mm × 15 mm glass substrate and then the monomer solution was sequentially spin-cast for another 12 s without stopping the rotation. The coated substrate was then rinsed in MeOH for 2 min and annealed on a hot plate at 110^{o}C for 10 min. Finally, a solid PEDOT film was obtained. The control sample was made by spin-coating PH1000 aqueous solution at 2000 r.p.m. on the 15 × 15 mm glass substrate and then dried at 110^{o}C for 10 min.

3. Sequential Solution Polymerize PEDOT on PET Film by Bar Coating

To reduce the viscosity of the oxidants solution, the MSA solution of V_2O_5 (supernatant) was diluted with MeOH and DMSO at a volume ratio of 5 : 4 : 1. Triton X-100 and Epoxy resin were added to tune the ink properties. Monomer solution was prepared by mixing chloroform with petroleum ether at 1 : 1 volume ratio, and then adding 10 vol % EDOT. The lower EDOT monomer concentration is helpful for decreasing the reaction rate and obtaining long polymer chains of PEDOTs. Video S1 showed the entire polymerization process. The oxidant solution was deposited on 15 cm × 12 cm PET films by bar coating. The coated film was immediately dipped into the monomer solution. The color of the film changed from yellow to blue within 1 s. Then the film was taken out and dipped in MeOH for 5 min. In the last step, the

film was dried at 110^{o}C for 10 min. The capacitive touch sensors were fabricated by the laser patterning the SSP PEDOT film on PET, which was then covered by Optically Clear Adhesive. The sensors (uncovered / covered with leather) were bonded with a controller and connected with a computer (or electric motor or light bulb) for touch function demonstrations.

4. Characterization

Electrical conductivity was measured using the Van der Pauw four-point probe technique with a Keithley 2400 source meter. Carrier concentration and carrier mobility were measured by a Hall Effect measurement system (Phys Tech, RH 2035). Film thickness was obtained using a Bruker Dektak XT stylus profiler. Atomic force microscopic (AFM) images were acquired using a multifunctional scanning probe microscope (MicroNano D-5A) in tapping mode. X-ray diffraction (PANalytical X'Pert Powder) was carried out to study the crystallinity of the samples, the 2θ scans were from 10° to 60°. Fourier transform infrared (FTIR) spectroscopy was recorded by ThermoFisher Nicolet FT-IR spectrometer (Nicolet iN10) in the range of 400 cm^{-1}~2000 cm^{-1}, the samples were prepared as KBr discs. X-ray photoelectron spectroscopy (XPS) was acquired using x-ray photoelectron spectrometer (ESCALAB 250Xi). Curve-fitting was carried out using XPS peak processing program (XPS PEAK 4.1), and the S2p signal was analyzed and deconvoluted compolents described by an envelope of Guessian-Lorentzian sum function with an asymmestry tail.(Zotti et al.,2003) Raman spectra were carried out by a laser Raman spectrometer (LabRAM HR Evolution), the curve-fitting of the Raman was carried out using XPS peak processing program (XPS PEAK 4.1) with assumption of 80% Gaussion and 20% Lorentzian component peaks. Absorption spectra of the films were recorded using UV-VIS-NIR spectrophotometer (UV-3600). Dynamic light scattering (DLS) data were obtained by Mastersizer 2000. In the DLS experiment, SSP PEDOT films were scraped off from the substrates and dispersed in DI water. The commercial solution of PH1000 was directly diluted 100 times by DI water. Both of the dispersions were treated with ultrasonication (2000 W) for 3 minutes before the DLS measurement. The sheet resistance of the SSP PEDOT films on flexible PET substrate was measured by a four-probe meter (DMR-1C).

Supplemental Reference

Zotti, G., Zecchin, S., Schiavon, G., Louwet, F., Groenendaal, L., Crispin, X., Osikowicz, W., Salaneck, W., and Fahlman, M. (2003). Electrochemical and XPS studies toward the role of monomeric and polymeric sulfonate counterions in the synthesis, composition, and properties of poly(3,4-ethylenedioxythiophene). Macromolecules *36*, 3337-3344.